

Received July 24, 2020, accepted August 10, 2020, date of publication August 20, 2020, date of current version September 11, 2020.

Digital Object Identifier 10.1109/ACCESS.2020.3018178

Multipoint-to-Multipoint Cooperative Multiuser SIM Free-Space Optical Communication: A Signal-Space Diversity Approach

ANSHUL JAISWAL¹, (Member, IEEE), MOHAMED ABAZA², (Senior Member, IEEE),
MANAV R. BHATNAGAR³, (Senior Member, IEEE),
AND RAED MESLEH⁴, (Senior Member, IEEE)

¹Department of Electronics and Communication Engineering, Indian Institute of Technology Roorkee, Roorkee 247667, India

²Department of Electronics and Communications Engineering, Arab Academy for Science, Technology and Maritime Transport, Giza 12577, Egypt

³Department of Electrical Engineering, Indian Institute of Technology Delhi, New Delhi 110016, India

⁴Electrical and Communication Engineering Department, School of Electrical Engineering and Information Technology, German Jordanian University, Amman 11180, Jordan

Corresponding author: Anshul Jaiswal (anshul.jaiswal@ece.iitr.ac.in)


ABSTRACT In this paper, a novel signal-space diversity (SSD) technique based multipoint-to-multipoint cooperative scheme for a multiuser free-space optical communication system is proposed. In SSD technique, constellation points of the transmitted signal are rotated by a certain angle and in-phase and quadrature components of two different symbols are interleaved to obtain diversity from the signal space. In the proposed scheme, the diversity of each cooperative user gets improved through joint encoding/decoding of the rotated symbols using subcarrier intensity modulation (SIM). The joint encoding/decoding can be done by connecting all the users' transceivers by wires that ensure the availability of the information of a user to all other users. The average symbol error rate for the proposed scheme under log-normal and gamma-gamma channel models is evaluated analytically and corroborated through Monte Carlo simulations. It is reported through intensive analyses and comparisons that the proposed cooperative scheme not only achieves full diversity order but also outperforms non-cooperative and repetition coding schemes.

INDEX TERMS Average symbol error rate, collaborative scheme, free-space optical communication, gamma-gamma channel, log-normal channel, subcarrier intensity modulation.

I. INTRODUCTION

Free-space optical (FSO) systems use very narrow laser beams, which enhances data security, allows high reuse factor without inducing interference, and improve robustness to electromagnetic interference. Moreover, FSO systems are license free, easy to deploy, and can be installed without the cost of digging fiber optic connections. As well, FSO systems are an efficient solution for the last mile problem to connect the end-user and the fiber optic infrastructure that already exist [1]. However, atmospheric turbulence (AT) or scintillation significantly degrades the performance of FSO systems [2], [3]. Therefore, various mitigation techniques for future FSO links are developed aiming to attain reliable high data-rate communications. Promising solutions include multiple-input multiple-output (MIMO) as well as distributed cooperative techniques. Most of the

investigated cooperative diversity methods involve point-to-point cooperative schemes. Serial relaying and parallel relaying are the two configurations of the point-to-point cooperative schemes. In the serial relaying configuration, the signal from source hops from one relay to another sequentially until it reaches destination [4], [5]. On the other hand, parallel relaying typically comprises the two path links, i.e., source-relays-destination and source-destination communication links. As such, it involves source-relay and relay-destination phases of communication. For both of the relaying configurations, amplify-and-forward (AF) is investigated in [6]–[10] while the decode-and-forward (DF) is examined in [6], [11]–[14]. However, due to the high directivity of the FSO system, schemes studied in [4]–[16] are not so popular as compared to their RF counterpart systems as described in [17]. Apart from point-to-point cooperative FSO systems, multiuser diversity (MD) in FSO systems has also been examined in [18]–[22]. The MD scheme is a point-to-multipoint scenario and comprises a central node

The associate editor coordinating the review of this manuscript and approving it for publication was Maurizio Magarini .

with K apertures that are employed to communicate with one of the K users. Some scheduling schemes are proposed in [18], where at a given time instant the central node serves the user with the largest channel gain. The work in [18] is extended in [19]–[21]. The MD scheduling schemes in [18]–[21] are based on single-input-single-output (SISO) FSO links. This work is extended to MIMO links in [22], where different scheduling protocols were compared over log-normal channel model.

Existing models of point-to-point FSO system in [4]–[16] and point-to-multipoint FSO system in [18]–[22] are similar to RF systems [23]–[25]. However, FSO systems are significantly different from RF systems. First, the nodes in an RF network can be mobile whereas FSO transceivers, in general, are static. Second, RF transmission is of broadcast nature, which is not possible in FSO system due to the high directivity of FSO transmitters. By exploiting these differences, the author in [17] proposed a new multipoint-to-multipoint FSO (M2M-FSO) specific cooperative system for intensity modulation/direct detection (IM/DD) process, where it is assumed that the FSO transceiver pairs are present on two buildings. In M2M-FSO system, N FSO transceiver pairs are placed on two buildings in order to establish N FSO connections for N different enterprises/users. The advantage of the scheme of [17] is that there is no latency and any user can access the channel at any time, which is a critical issue in the MD scheduling schemes proposed in [18]–[22]. Besides, M2M-FSO is significantly different from traditional MIMO techniques. In traditional MIMO techniques, the receiver apertures are very close to each other (order of centimeters); therefore, the signals transmitted by a transmit aperture are detected by all receive apertures. This does not happen in M2M-FSO scheme where several meters of the distance exists between different FSO transmitters/receivers. Also, in [17], a collaborative scheme is proposed where the transceivers installed in the same building are connected by means of wires. Using this connection, users can exchange their data among each other in order to gain some collaborative diversity. More specifically, N users are clustered in a number of groups and all users in a group transmit an encoded symbol simultaneously. It is reported in [17] that the performance of the clustered-based M2M-FSO scheme is highly dependent on the user grouping. Due to the grouping of users, the error performance of the users of a particular group is different than the users of other groups. To overcome the problem of determining the optimal grouping for different number of users and different error performance for different users, a novel cooperative scheme is proposed in this paper. The idea is to use signal space diversity (SSD) technique instead of groups clustering. SSD improves the diversity order by exploiting the modulation signal space [26]. Thereby, the problems of finding the optimal grouping for different number of users and the different error performance for different users is completely eliminated. Note that SSD is completely different from space shift keying (SSK) [27], [28]. In SSK, only one light source

is activated at a time based on the incoming data bits while SSD rotates the constellation points.

With reference to existing literature, the main contributions of this paper are as follows:

- A novel SSD-based M2M-FSO specific cooperative scheme is presented and analysed under log-normal and gamma-gamma channel models for multiple users using different modulation levels.
- In order to use SSD, the proposed scheme employs subcarrier intensity modulation (SIM) technique.
- The analytical expressions of the average symbol error rate (ASER) for the proposed scheme under the considered channel models are evaluated and substantiated through Monte Carlo simulations.
- The optimal SSD rotation angles at which the error performance is minimum are also investigated under different turbulence regimes and modulation orders.
- Comparisons of the proposed collaborative set-up with non-cooperative and repetition coding (RC) set-up are presented.

Many useful outcomes are seen from the thorough analyses of the proposed cooperative scheme. The foremost inference is that the diversity order gained by each user increases by collaborating with other users. This means that a higher number of collaborative users will lead to better performance for each user.

The rest of the paper is organized as follows. Section II introduces the preliminaries of the work which includes the system model, channel model, and the proposed strategy. The framework to derive ASER of the proposed SSD-based M2M-FSO system under log-normal and gamma-gamma channel models is presented in Section III. Numerical results are discussed in Section IV, and Section V concludes the paper.

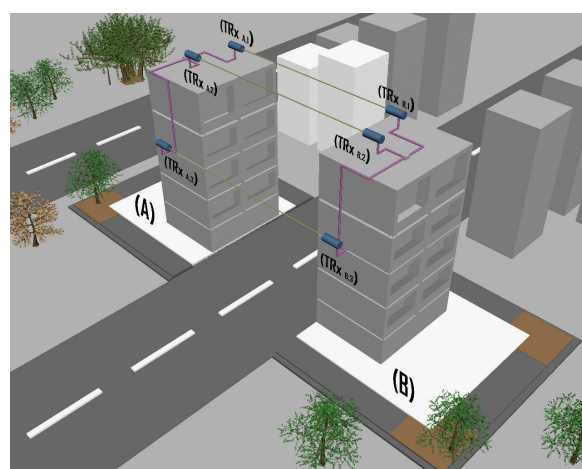


FIGURE 1. System model of the proposed M2M-FSO system.

II. PRELIMINARIES

A. SYSTEM MODEL AND PROPOSED COOPERATIVE STRATEGY

The system model of the proposed M2M-FSO system for N users is depicted in Fig. 1. There are N FSO transceivers

mounted on building rooftops or under windows in order to realize connectivity between two distant locations A and B . Since FSO connections are highly directive, a distinct pair of FSO transceivers is dedicated to each user to communicate. However, using dedicated FSO link by a single user (which is called M2M non-cooperation FSO (M2M-NC-FSO) scheme) achieves no diversity gain. Therefore, [17] proposed a new multipoint-to-multipoint cooperative FSO (M2M-C-FSO) scheme where, all the transceivers of the same building are connected by wires to ensure the availability of information of a user to all other users as shown in Fig. 1. This allows joint encoding/decoding in the M2M-FSO scheme with a cost-effective approach where the existing infrastructure of M2M-NC-FSO is used. Furthermore, the channels are uncorrelated as inter-transmitter and inter-receiver spacing are very large as shown in Fig. 1.

The system model of the proposed scheme in this paper is the same as that given in [17]. However, significant alterations have been done in the existing strategy of cooperation *to improve the performance of each user and to reduce design complexity as compared to [17]*. The point-wise differences between these two cooperative strategies are as follows:

- In [17], N users are divided into a number of groups. All users of a given group transmit the same encoded symbol, which comprises the information of all the users of that group. The encoded symbols are nothing but the higher order modulation symbols, whose modulation order is higher than the modulation order of the users' symbols. In the proposed scheme, there is no need to divide the users into a number of groups. Also, the modulation order of the encoded symbol will be the same as that of the modulation order of the users' symbols irrespective of the number of users.
- Due to the grouping of users, different classes of service have been introduced for different users in [17]. The users have been classified as gold users, silver users, bronze users, etc. according to the diminishing error performance. Therefore, the performance is highly dependent on the user grouping and the search for optimal grouping adds an extra design complexity in [17]. In the proposed scheme, all users are gold users and achieve the best error performance.
- In [17], the partitioning of the N users into different groups depends on the values of the channel gains. More specifically, information about the order of channel gain has to be sent periodically to the transmitter side. The transmitter uses this information to regroup the users based on new channel states. On the other hand, since the performance of the proposed strategy is independent of channel states, there is no need to periodically send channel state information which significantly reduces overall design complexity.
- The analytical framework presented in [17] only provides *asymptotic* error performance under the gamma-gamma channel model, while the analytical framework presented in our work gives a *general* error

performance which can be further used to obtain the asymptotic error performance. In addition, our work also provides the performance analysis of the considered system in log-normal channel model.

- In [17], the diversity order is improved by transmitting the jointly encoded symbols simultaneously from all the users of the group. However, in the proposed cooperative scheme, the diversity order will be improved by using the concept of SSD technique.
- The transmission technique used in [17] is the intensity modulation and direct detection, while this work employs the SIM technique.

All the above points explicate that the proposed M2M-C-FSO scheme is completely different from [17] according to the strategic and analytical framework. This inspires a separate investigation of the proposed scheme.

B. SSD TECHNIQUE

Before going into the details of the proposed cooperative strategy, let us introduce the concept of SSD briefly. The SSD is a technique of enhancing the diversity order by exploiting the modulation signal space [26]. As an example, for a 2-dimensional signal constellation, both the in-phase and the quadrature components of the transmitted signal should have enough information to uniquely represent the original signal. This can be achieved through rotating the constellation symbols by a certain angle prior to transmission. An example of quadrature phase shift keying (QPSK) is illustrated in Fig. 2. It can be observed from the figure that after rotating with θ degrees, the in-phase and the quadrature components of each symbol *individually* carry enough information to uniquely represent the symbol. Now, if in-phase and quadrature components of the signal are transmitted through independent paths, the overall diversity order of the system will be improved.

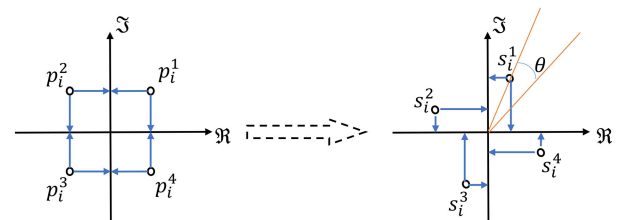


FIGURE 2. Conventional QPSK constellation and Rotated QPSK constellation.

The proposed M2M-C-FSO strategy to improve the system performance can be understood briefly with the following steps:

- The users first share their rotated M -ary phase shift keying (M -PSK) symbol (which needs to be transferred to the destination) with all other users.
- Using interleaving, the symbols from different users are jointly encoded in some predefined manner to form a new symbol termed as *cooperative symbol*.

More specifically, the in-phase and quadrature component of the cooperative symbol contains information about two different users.

- The generated cooperative symbol at each transmitter node is then transmitted through the FSO link.
- At the receiver, the symbol of a particular user is estimated using maximum-likelihood (ML) detector by processing of all the received cooperative symbols.

To understand the proposed strategy, we will first discuss an elementary set-up of M2M-C-FSO for two users in the next subsection.

C. THE PROPOSED M2M-C-FSO SCHEME FOR TWO USERS

Let us consider two LASER-based set-up which will be used by two users. Under the non-cooperative scenario, both users utilize different FSO links and a limited diversity order of the SISO system can be achieved. On the other hand, in the proposed cooperative scheme, the SSD technique is used to enhance the diversity. The schematic of the two-user M2M-C-FSO scheme is illustrated in Fig. 3. To describe the information flow in the M2M-C-FSO system, let us consider an example using the QPSK modulation scheme:

- 1) Let us consider p_1 and p_2 are the classical QPSK symbols of user 1 and 2 respectively, where $p_i \in (p_i^1, p_i^2, p_i^3, p_i^4)$, $i = 1, 2$, as in Fig. 2.
- 2) After a rotation of θ degrees, a new constellation $s_i \in (s_i^1, s_i^2, s_i^3, s_i^4)$ is created, known as rotated QPSK. The mathematical relation between these constellation points can be given by

$$\begin{bmatrix} s_i^1 \\ s_i^3 \\ s_i^2 \\ s_i^4 \end{bmatrix} = \begin{bmatrix} p_i^1 & p_i^2 \\ p_i^3 & p_i^4 \end{bmatrix} \begin{bmatrix} \cos(\theta) & -\sin(\theta) \\ \sin(\theta) & \cos(\theta) \end{bmatrix} \quad (1)$$

The SSD module shown in Fig. 3 converts the p_i into s_i by using (1).

- 3) The rotated QPSK symbol is then made available at other transmitters by using connecting wires. Using interleaving at the transmitter side, the rotated QPSK signal of user 1 and user 2 are combined as follows:

$$c_1 = \Re(s_1) + j\Im(s_2), \quad (2)$$

$$c_2 = \Re(s_2) + j\Im(s_1), \quad (3)$$

where c_1 and c_2 are the cooperative symbols that contain the signal components of both the users.

- 4) The symbol c_1 is communicated through the first transceiver pair, whereas c_2 is transmitted through the second transceiver pair. Since c_1 and c_2 are complex signals, we have to use the subcarrier intensity modulation (SIM) technique to transfer these symbols through FSO links [29], [30]. For SIM-based FSO link, the received electrical current for the receiver related to user i can be written as

$$i_i(t) = PRh_i(1 + \xi c_i(t)) + n_i(t), \quad (4)$$

where P is the average transmitter power, R is the responsivity of the photo-detector, $h_i \triangleq h_{ii}$ is the

instantaneous channel gain of the i^{th} FSO link, $n_i(t)$ is the zero mean complex additive white Gaussian noise with σ_n^2 variance, ξ is the modulation index, and $c_i(t)$ is given by [31]

$$c_i(t) = \Re(c_i(t)) \cos(2\pi f_c t) - \Im(c_i(t)) \sin(2\pi f_c t), \quad (5)$$

where $\Re(c_i(t)) = \sum_l g(t - lT_s) \cos(\phi_l)$ is the in-phase signal, $\Im(c_i(t)) = \sum_l g(t - lT_s) \sin(\phi_l)$ is the quadrature signal, ϕ_l is the l^{th} phase symbol, $g(t)$ is the shaping pulse, and T_s is the symbol time. In order to avoid non-linearity, the amplitude satisfies $\sqrt{(\Re(c_i(t)))^2 + (\Im(c_i(t)))^2} \leq 1$. Also, to keep the optical transmitter within its dynamic range and to avoid over-modulation induced clipping, $\xi c_i(t) \leq 1$ is considered. The received signal is then passed through the bandpass filter followed by down conversion. After carrier recovery and sampling at sampling rate, the output signal y_i is given as

$$y_i = PR\xi h_i c_i + n_i. \quad (6)$$

Since c_i contains the information of both users, the output signal of the demodulator also has the information of both users. For example, the in-phase and quadrature components of the received signal y_1 are

$$\Re(y_1) = PR\xi h_1 \Re(s_1) + \Re(n_1) \quad (7)$$

and

$$\Im(y_1) = PR\xi h_1 \Im(s_2) + \Im(n_1), \quad (8)$$

respectively. Therefore, the in-phase of y_1 contains the information of user 1 whereas, its quadrature has the information of user 2. By deinterleaving, the in-phase and quadrature parts of the received signal y_i can be separated and processed individually.

- 5) Finally, the following ML detection rules are used to estimate the transmitted symbols:

$$\hat{s}_1 = \arg \min_{s_1 \in S} \left[(\Re(y_1) - PR\xi h_1 \Re(s_1))^2 + (\Im(y_1) - PR\xi h_2 \Im(s_1))^2 \right], \quad (9)$$

and

$$\hat{s}_2 = \arg \min_{s_2 \in S} \left[(\Re(y_2) - PR\xi h_2 \Re(s_2))^2 + (\Im(y_2) - PR\xi h_1 \Im(s_2))^2 \right]. \quad (10)$$

From the above detection rules, it is clear that the estimation of any of the symbols requires both received signals. Therefore, all the receiver nodes should be connected with wires such that all received signals are available at each receiver node. The presence of both channel gains in the ML detection given in (9) and (10) indicates that the considered two users system will have double diversity order as compared to the non-cooperative system.

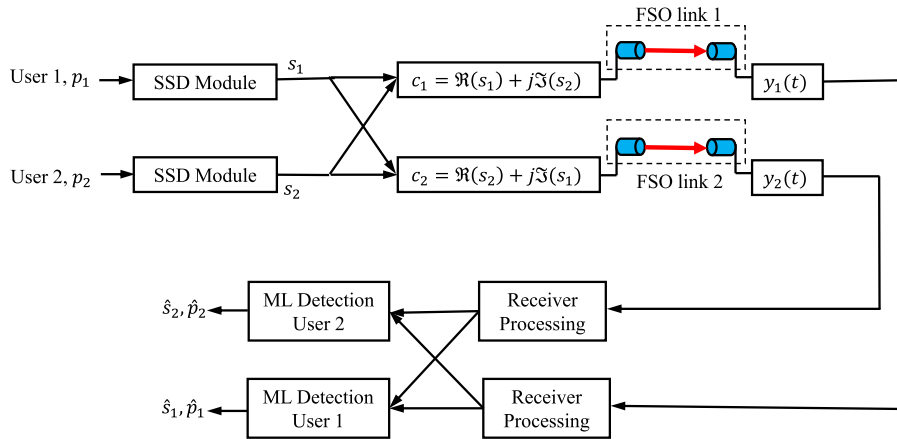


FIGURE 3. Two-user based M2M-C-FSO system.

Note that the proposed system can also employ the M -ary PSK symbol. For M -ary PSK, the search given in (9) and (10) will be for M symbols.

D. INSTANTANEOUS SER

For the i^{th} user, the upper bound SER of the proposed scheme employing M -PSK modulation can be obtained by summing all pair-wise error probabilities (PEPs) as

$$SER_i^U \leq \frac{1}{|S|} \sum_j \sum_{k \neq j} PEP^{s_i^j \rightarrow s_i^k}, \quad (11)$$

where s_i^j denotes the j^{th} , $1 \leq j \leq M$, symbol of i^{th} user constellation and $PEP^{s_i^j \rightarrow s_i^k}$ is the PEP for the symbol s_i^j when detected as $s_i^k \neq s_i^j$.

Lemma 1: The PEP expression for the first user based on ML detector given in (9) is given by

$$PEP^{s_1^j \rightarrow s_1^k} = Q\left(\sqrt{\frac{\gamma}{2} \left[h_1^2 (\Re(\hat{s}_1^k) - \Re(s_1^j))^2 + h_2^2 (\Im(\hat{s}_1^k) - \Im(s_1^j))^2 \right]}\right), \quad (12)$$

where $\gamma = P^2 R^2 \xi^2 / \sigma_n^2$ is the signal-to-noise (SNR) ratio per symbol and $Q(\cdot)$ is the Gaussian Q-function.

Proof: Refer to Appendix A for the proof.

Similar to user 1, the SER for user 2 can be obtained from (10), which can be expressed as

$$PEP^{s_2^k \rightarrow s_2^j} = Q\left(\sqrt{\frac{\gamma}{2} \left[h_2^2 (\Re(\hat{s}_2^k) - \Re(s_2^j))^2 + h_1^2 (\Im(\hat{s}_2^k) - \Im(s_2^j))^2 \right]}\right). \quad (13)$$

The upper bound SER of the overall system can then be obtained as

$$SER^U \leq 1 - \prod_i (1 - SER_i^U). \quad (14)$$

The SER expressions given in (11) and (14) are the generalized expression and not limited to 2 users. This means for N users, the value of i will range from 1 to N .

E. CHANNEL MODEL

In this work, two different channel models of intensity fluctuation are considered to cover weak-to-strong turbulence regimes. The probability density function (pdf) of these two channel models are discussed hereinafter.

1) LOG-NORMAL CHANNEL

The log-normal pdf is given by [32]

$$f_{h_i}(h_i) = \frac{1}{h_i \sqrt{8\pi\sigma^2}} \exp\left(-\frac{(\ln(h_i) - 2\mu)^2}{8\sigma^2}\right), \quad (15)$$

where $h_i = \exp(2X)$ is the channel coefficient with X being an independent and identically distributed (i.i.d.) Gaussian random variable (RV) with mean μ , standard deviation σ , and variance σ^2 . To ensure that the fading channel does not attenuate or amplify the average power, the fading coefficients are normalized as $\mathbf{E}[h_i^2] = e^{2(\mu + \sigma^2)} = 1$. This model is used to characterize the weak turbulence condition.

2) GAMMA-GAMMA CHANNEL

For moderate-to-strong regime, h_i is modelled as a Gamma-Gamma distributed RV with the following pdf:

$$f_{h_i}(h_i) = \frac{(\alpha\beta)^{\frac{\alpha+\beta}{2}}}{\Gamma(\alpha)\Gamma(\beta)} h_i^{\frac{\alpha+\beta}{2}-1} G_{0,2}^{2,0}\left(\alpha\beta h_i \left| \frac{\alpha-\beta}{2}, \frac{\beta-\alpha}{2} \right.\right), \quad (16)$$

where $G_{p,q}^{m,n}[\cdot]$ is the Meijer's G -function [33, Eq.(9.301)],¹ $\Gamma(\cdot)$ is the Gamma function [33, Eq. (8.310)], α and β are the effective number of large-scale and small-scale eddies of scattering environment, respectively, and they are related according to Rytov variance (σ_I^2).

¹The Meijer-G function is a standard built-in function available in most popular mathematical software packages, such as Maple and Mathematica.

III. PROPOSED COOPERATIVE SCHEME FOR N USERS

An apparent extension of the proposed scheme according to [17] for N users scenario, i.e., for $N \times N$ system, is by employing N -dimensional modulation scheme. This however entails that whenever the number of users changes, the modulation dimension for each user should be modified accordingly. Adjusting modulation dimension depending on the number of active users demands significant changes in hardware and signal processing levels at both the transmitter and receiver units. Therefore for the sake of simplicity, we propose a space-time layer that is easier to implement than changing the modulation order and dimension. The upcoming subsections explain the proposed scheme for arbitrary number of users. More specifically, ML detection, SER, and ASER of N users SSD-based M2M-C-FSO scheme will be presented hereinafter.

A. ML DETECTION AND SER OF N USERS M2M-C-FSO SCHEME

Using the concept of cooperative scheme for two users as discussed in the previous section, the cooperation scheme for N users can be established. For N users, an space time block code (STBC) structure of $N \times \lceil N/2 \rceil$ size as given in (17), as shown at the bottom of the page is proposed, which is nothing but the combination of cooperative symbols as discussed for 2 user M2M-C-FSO system in Subsection II-C, where $\lceil \cdot \rceil$ denotes a ceiling function. The difference in STBC structure for odd and even number of users is given in the last column as illustrated in (17). The ML detection for user 1 for the given

STBC is as follows:

$$\hat{s}_1 = \arg \min_{s_1 \in \mathcal{S}} \left[\sum_{m=1}^{\lceil N/2 \rceil} (\Re(y_{2m-1}(m)) - PR\xi h_{2m-1} \Re(s_1))^2 + (\Im(y_N(1)) - PR\xi h_N \Im(s_1))^2 + u(N-3) \sum_{m=1}^{\lceil N/2 \rceil - 1} (\Im(y_{2m}(m+1)) - PR\xi h_{2m} \Im(s_1))^2 \right], \tag{18}$$

where $y_{n_r}(t)$ is the received signal at $1 \leq n_r^{th} \leq N$ receiver at $1 \leq t^{th} \leq \lceil N/2 \rceil$ time interval, and $u(n)$ is defined as:

$$u(n) \triangleq \begin{cases} 1, & n \geq 0, \\ 0, & n < 0. \end{cases} \tag{19}$$

Now, using a framework similar to the one employed in Subsection III-A, the PEP between s_1^j and s_1^k for the above ML detector can be derived and it is given in (20), as shown at the bottom of the page, where

$$\delta(n) \triangleq \begin{cases} 1, & n = 0, \\ 0, & n \neq 0. \end{cases} \tag{21}$$

Since the argument of the Q-function in (20) has N number of h^2 terms, the proposed N user collaborative scheme will have N times higher diversity order as compared to non-collaborative scheme. For better representation, we have modified (20) into (22), as shown at the bottom of the page, where $A_{kj} = (\Re(s_1^k) - \Re(s_1^j))^2$ and $B_{kj} = (\Im(s_1^k) - \Im(s_1^j))^2$.

Column 1	Column 2	...	Column $N/2$, for even N	Column $\lceil N/2 \rceil$, for odd N
$\Re(s_1) + j\Im(s_2)$	$\Re(s_{N-1}) + j\Im(s_N)$...	$\Re(s_3) + j\Im(s_4)$	$\Re(s_2) + j\Im(s_3)$
$\Re(s_2) + j\Im(s_3)$	$\Re(s_N) + j\Im(s_1)$...	$\Re(s_4) + j\Im(s_5)$	$\Re(s_3) + j\Im(s_4)$
\vdots	$\Re(s_1) + j\Im(s_2)$	\ddots	\vdots	\vdots
\vdots	$\Re(s_2) + j\Im(s_3)$	\ddots	\vdots	\vdots
\vdots	\vdots	\ddots	\vdots	\vdots
\vdots	\vdots	\ddots	$\Re(s_{N-1}) + j\Im(s_N)$	\vdots
\vdots	\vdots	\ddots	$\Re(s_N) + j\Im(s_1)$	$\Re(s_{N-1}) + j\Im(s_N)$
$\Re(s_{N-1}) + j\Im(s_N)$	$\Re(s_{N-3}) + j\Im(s_{N-2})$...	$\Re(s_1) + j\Im(s_2)$	$\Re(s_N) + j\Im(s_1)$
$\Re(s_N) + j\Im(s_1)$	$\Re(s_{N-2}) + j\Im(s_{N-1})$...	$\Re(s_2) + j\Im(s_3)$	$\Re(s_1) + j\Im(s_2)$

$\left. \right] \tag{17}$

$$PEP^{s_1^j \rightarrow s_1^k} = Q \left(\sqrt{\frac{\gamma}{2} \left[\left(\sum_{m=1}^{\lceil N/2 \rceil} h_{2m-1}^2 \right) (\Re(s_1^k) - \Re(s_1^j))^2 + \left(\sum_{m=1}^{\lfloor N/2 \rfloor} \left[h_{2m}^2 + h_N^2 \delta(N - (2m + 1)) \right] \right) (\Im(s_1^k) - \Im(s_1^j))^2 \right]} \right). \tag{20}$$

$$PEP(A_{kj}, B_{kj}) = Q \left(\sqrt{\frac{\gamma}{2} \left[A_{kj} \sum_{m=1}^{\lceil N/2 \rceil} h_{2m-1}^2 + B_{kj} \left(\sum_{m=1}^{\lfloor N/2 \rfloor} \left[h_{2m}^2 + h_N^2 \delta(N - (2m + 1)) \right] \right) \right]} \right). \tag{22}$$

B. ASER EXPRESSIONS OF THE PROPOSED COOPERATIVE SCHEME

The mathematical expression of the ASER for the proposed scheme based on (18) is calculated under different channel models in the following subsection.

1) LOG-NORMAL DISTRIBUTION

The APEP of (22) can be determined by solving the integral in (23), as shown at the bottom of the page. In (23),

$$\gamma_k = \gamma h_k^2, \quad 1 \leq k \leq N \quad (24)$$

is the instantaneous SNR of the k^{th} link and h_k is distributed according to log-normal channel distribution. After a few algebraic manipulations, the pdf of γ_k can be given by

$$f(\gamma_k) = \frac{1}{\sqrt{32\pi\sigma^2\gamma_k}} \exp\left[-\frac{\left(\ln\left(\frac{\gamma_k}{\gamma}\right) + 4\sigma^2\right)^2}{32\sigma^2}\right]. \quad (25)$$

According to [34], the moment generating function is defined as

$$\Psi(s') \triangleq \int_0^\infty \dots \int_0^\infty f(\gamma_1) \dots f(\gamma_N) \times \exp\left[-\sum_{i=1}^N s'_i \gamma_i\right] d\gamma_1 \dots d\gamma_N. \quad (26)$$

Substitute (25) in (26) and using the relation

$$\int_{-\infty}^\infty \exp(-x^2)g(x)dx \approx \sum_{l=1}^M w_l g(x_l), \quad (27)$$

yields

$$\Psi(s') \approx \sum_{m_1=1}^M \dots \sum_{m_N=1}^M \left[\prod_{i=1}^N \frac{w_{m_i}}{\sqrt{\pi}} \right] \times \exp\left[-\sum_{j=1}^N s'_j \gamma \exp\left(\sqrt{32\sigma^2 x_{m_j}} - 4\sigma^2\right)\right], \quad (28)$$

where M is the order of approximation of the Hermite polynomial. The values of w_{m_i} and x_{m_j} of the M^{th} order Hermite polynomial are tabulated in [33, Table 25.10]. An alternative form of the Gaussian-Q function is

$$Q(y) = \frac{1}{\sqrt{2\pi}} \int_y^\infty \exp\left(-\frac{x^2}{2}\right) dx = \frac{1}{\pi} \int_0^{\frac{\pi}{2}} \exp\left(-\frac{y^2}{2\sin^2\theta}\right) d\theta. \quad (29)$$

Using the alternative definition of the Q-function in (29) on (23) and using (26) yields,

$$\text{APEP}(A_{kj}, B_{kj}) \approx \frac{1}{\pi} \int_0^{\frac{\pi}{2}} \Psi\left(\frac{A_{kj}\gamma I_1 + B_{kj}\gamma I_2}{4\sin^2(\theta)}\right) d\theta, \quad (30)$$

where

$$I_1 = \left[\sum_{j=1}^{\lceil N/2 \rceil} \exp\left(\sqrt{32\sigma^2 x_{m(2j-1)}} - 4\sigma^2\right) \right] \quad (31)$$

and

$$I_2 = \left[\sum_{k=1}^{\lfloor N/2 \rfloor} \left[\exp\left(\sqrt{32\sigma^2 x_{m(2k)}} - 4\sigma^2\right) + \delta(N - (2k + 1)) \exp\left(\sqrt{32\sigma^2 x_{m(N)}} - 4\sigma^2\right) \right] \right], \quad (32)$$

which is solved by (28) after few manipulations as

$$\text{APEP}(A_{kj}, B_{kj}) \approx \sum_{m_1=1}^M \dots \sum_{m_N=1}^M \left[\prod_{i=1}^N \frac{w_{m_i}}{\sqrt{\pi}} \right] \times Q\left(\sqrt{\frac{1}{2} [A_{kj}\gamma I_1 + B_{kj}\gamma I_2]}\right). \quad (33)$$

Now, by substituting (33) into (11), ASER of the overall system can be obtained.

Example: For QPSK symbol, the SER of the proposed scheme for the user 1 in an N users system can be obtained by (11) as

$$\begin{aligned} \text{SER}_1^U &\leq \frac{1}{4} \sum_j \sum_{k \neq j} \text{PEP}^{s_j^1 \rightarrow \hat{s}_1^k} \\ &= \frac{2}{4} \sum_j \sum_{k=j+1} \text{PEP}^{s_j^1 \rightarrow \hat{s}_1^k} \\ &= \frac{1}{2} (\text{PEP}^{s_1^1 \rightarrow \hat{s}_1^2} + \text{PEP}^{s_1^1 \rightarrow \hat{s}_1^3} + \text{PEP}^{s_1^1 \rightarrow \hat{s}_1^4} + \text{PEP}^{s_2^1 \rightarrow \hat{s}_1^3} \\ &\quad + \text{PEP}^{s_2^1 \rightarrow \hat{s}_1^4} + \text{PEP}^{s_3^1 \rightarrow \hat{s}_1^4}), \end{aligned} \quad (34)$$

where $s_1^1 = (\cos\theta - \sin\theta)/\sqrt{2} + j(\cos\theta + \sin\theta)/\sqrt{2}$, $s_1^2 = -(\cos\theta + \sin\theta)/\sqrt{2} + j(\cos\theta - \sin\theta)/\sqrt{2}$, $s_1^3 = (\sin\theta - \cos\theta)/\sqrt{2} - j(\cos\theta + \sin\theta)/\sqrt{2}$, $s_1^4 = (\sin\theta + \cos\theta)/\sqrt{2} - j(\sin\theta - \cos\theta)/\sqrt{2}$.

By using (20), the PEPs of the considered system can be calculated and represented in the form of (22) as

$$\begin{aligned} \text{PEP}^{s_1^1 \rightarrow \hat{s}_1^2} &= \text{PEP}^{s_1^3 \rightarrow \hat{s}_1^4} = \text{PEP}(2\cos^2\theta, 2\sin^2\theta) \\ \text{PEP}^{s_1^1 \rightarrow \hat{s}_1^4} &= \text{PEP}^{s_2^1 \rightarrow \hat{s}_1^3} = \text{PEP}(2\sin^2\theta, 2\cos^2\theta) \\ \text{PEP}^{s_1^1 \rightarrow \hat{s}_1^3} &= \text{PEP}(2(\cos\theta - \sin\theta)^2, 2(\cos\theta + \sin\theta)^2) \\ \text{PEP}^{s_2^1 \rightarrow \hat{s}_1^4} &= \text{PEP}(2(\cos\theta + \sin\theta)^2, 2(\cos\theta - \sin\theta)^2) \end{aligned} \quad (35)$$

$$\text{PEP}(A_{kj}, B_{kj}) = \int_0^\infty \dots \int_0^\infty Q\left(\sqrt{\frac{1}{2} \left[A_{kj} \sum_{m=1}^{\lceil N/2 \rceil} \gamma_{2m-1} + B_{kj} \sum_{m=1}^{\lfloor N/2 \rfloor} \left[\gamma_{2m} + \gamma_N \delta(N - (2m + 1)) \right] \right]}\right) \prod_{m=1}^N f(\gamma_m) \prod_{m=1}^N d\gamma_m. \quad (23)$$

Using (33), the average of each PEPs given in (35) can be evaluated. Furthermore, assuming even number N , $\text{PEP}(A_{kj}, B_{kj}) = \text{PEP}(B_{kj}, A_{kj})$, which implies

$$\begin{aligned} \text{APEP}^{s_1 \rightarrow \hat{s}_1^2} &= \text{APEP}^{s_1 \rightarrow \hat{s}_1^4} = \text{APEP}^{s_1 \rightarrow \hat{s}_1^4} \\ &= \text{APEP}^{s_1^2 \rightarrow \hat{s}_1^3} = \text{APEP}(2 \cos^2 \theta, 2 \sin^2 \theta), \\ \text{APEP}^{s_1 \rightarrow \hat{s}_1^3} &= \text{APEP}^{s_1^2 \rightarrow \hat{s}_1^4} \\ &= \text{APEP}(2(\cos \theta - \sin \theta)^2, 2(\cos \theta + \sin \theta)^2). \end{aligned} \quad (36)$$

Consequently, the ASER of the considered example can be calculated using (34) and (36) as

$$\text{ASER}_1^U \leq 2\text{APEP}^1 + \text{APEP}^2, \quad (37)$$

where $\text{APEP}^1 = \text{APEP}(2 \cos^2 \theta, 2 \sin^2 \theta)$ and $\text{APEP}^2 = \text{APEP}(2(\cos \theta - \sin \theta)^2, 2(\cos \theta + \sin \theta)^2)$.

2) GAMMA-GAMMA CHANNEL

An alternative way to determine the APEP is by solving the following integral:

$$\text{APEP}(A_{kj}, B_{kj}) = \int_0^\infty Q\left(\sqrt{\frac{\gamma z}{2}}\right) f_Z(z) dz, \quad (38)$$

where

$$z = A_{kj} \sum_{m=1}^{\lfloor N/2 \rfloor} h_{2m-1}^2 + B_{kj} \sum_{m=1}^{\lfloor N/2 \rfloor} (h_{2m}^2 + h_N^2 \delta(N - (2m + 1))). \quad (39)$$

Therefore, in order to find the APEP using (38), the distribution of the RV z is needed. Since the diversity order of any scheme depends on the number of h^2 terms in the Q-function, the removal of h_N^2 from second summation in (39) will not affect the diversity order since the same term is already present in the first summation. More specifically, the sub-optimal detector for odd number of users can be written as

$$\begin{aligned} \hat{s}_1 = \arg \min_{s_1 \in S} & \left[\sum_{m=1}^{\lfloor N/2 \rfloor} (\Re(y_{2m-1}(m)) - PR\xi h_{2m-1} \Re(s_1))^2 \right. \\ & \left. + u(N - 3) \sum_{m=1}^{\lfloor N/2 \rfloor - 1} (\Im(y_{2m}(m + 1)) - PR\xi h_{2m} \Im(s_1))^2 \right]. \end{aligned} \quad (40)$$

This will provide the same diversity order as provided by ML given in (18). Based on (40), the APEP can be derived by solving the following relation:

$$\text{APEP}(A_{kj}, B_{kj}) = \int_0^\infty Q\left(\sqrt{\frac{\gamma z'}{2}}\right) f_{Z'}(z') dz', \quad (41)$$

where

$$z' = A_{kj} \sum_{m=1}^{\lfloor N/2 \rfloor} h_{2m-1}^2 + B_{kj} \sum_{m=1}^{\lfloor N/2 \rfloor} h_{2m}^2 = w_{A_{kj}} + w_{B_{kj}}, \quad (42)$$

with $w_{A_{kj}} = A_{kj} \sum_{m=1}^{\lfloor N/2 \rfloor} h_{2m-1}^2$ and $w_{B_{kj}} = B_{kj} \sum_{m=1}^{\lfloor N/2 \rfloor} h_{2m}^2$. It can be easily shown that for even number of users $z' = z$. Therefore, (41) can also be used to determine the APEP for even number of users. Since gamma-gamma channel distribution is quite complex, for the sake of simplicity, (41) will be solved instead of (38). It is obvious that for odd number of users, the ASER derived from sub optimal detector is higher than optimal detector, but the diversity order will be the same for both detectors. However, the difference in coding gain between the ASERs of optical ML and sub-optimal ML is marginal (about 1 dB). This will be discussed in details in Section V.

Lemma 2: The pdf of the RV z' is given by

$$\begin{aligned} f_{Z'}(z') &= \sum_{m_1=0}^{N_1} \sum_{m_2=0}^{N_2} \binom{N_1}{m_1} \binom{N_2}{m_2} \\ &\times \sum_{q=0}^{\infty} G_q(N_1, N_2, m_1, m_2, A_{kj}, B_{kj}) \\ &\times \frac{z'^{\frac{q+(N_1+N_2-m_1-m_2)\beta+(m_1+m_2)\alpha}{2}}}{\Gamma\left(\frac{q+(N_1+N_2-m_1-m_2)\beta+(m_1+m_2)\alpha}{2}\right)}, \end{aligned} \quad (43)$$

where

$$\begin{aligned} G_q(N_1, N_2, m_1, m_2, A_{kj}, B_{kj}) &= E_q(N_1, m_1, A_{kj}) * E_q(N_2, m_2, B_{kj}), \\ E_q(N_1, m_1, A_{kj}) &= c_q(N_1 - m_1, m_1) / (A_{kj}^{\frac{q+(N_1-m_1)\beta+m_1\alpha}{2}}), \\ c_q(\mu, \nu) &= b_q^{(\mu)}(\alpha, \beta) * b_q^{(\nu)}(\beta, \alpha), \\ b_q(\alpha, \beta) &= \frac{a_q(\alpha, \beta)}{2} \Gamma\left(\frac{q + \beta}{2}\right), \\ a_q(\alpha, \beta) &= \frac{(\alpha\beta)^{\beta+q} \Gamma(\alpha - \beta)}{\Gamma(\alpha)\Gamma(\beta)(1 + \beta - \alpha)q!}, \end{aligned} \quad (44)$$

and $N_1 = \lfloor N/2 \rfloor$, $N_2 = \lfloor N/2 \rfloor$, and $b_q^{(\mu)}(\alpha, \beta)$ denotes $b_q(\alpha, \beta)$ is convolved with $\mu - 1$ times with itself, e.g. $b_q^{(2)}(\alpha, \beta) = b_q(\alpha, \beta) * b_q(\alpha, \beta)$. Also, $b_q^{(0)}(\alpha, \beta) = 1$.

Proof: Refer to Appendix B for the proof.

On substituting (43) into (41) and using the relation [27, Eq. (48)], the APEP can be obtained as

$$\begin{aligned} \text{APEP}(A_{kj}, B_{kj}) &= \sum_{m_1=0}^{N_1} \sum_{m_2=0}^{N_2} \binom{N_1}{m_1} \binom{N_2}{m_2} \\ &\times \sum_{q=0}^{\infty} \frac{G_q(N_1, N_2, m_1, m_2, A_{kj}, B_{kj})}{\Gamma\left(\frac{q+(N_1+N_2-m_1-m_2)\beta+(m_1+m_2)\alpha}{2}\right)} \\ &\times \frac{1}{\Gamma\left(\frac{q+(N_1+N_2-m_2-m_1)\beta+(m_1+m_2)\alpha}{2}\right)} \\ &\times \frac{1}{(q + (N_1 + N_2 - m_2 - m_1)\beta + (m_1 + m_2)\alpha)} \\ &\times \frac{1}{\sqrt{\pi} \left(\frac{\sqrt{\gamma}}{2}\right)^{q+(N_1+N_2-m_2-m_1)\beta+(m_1+m_2)\alpha}}. \end{aligned} \quad (45)$$

Now, by substituting (45) into (11), ASER of the overall system can be obtained. Following the same procedure as in (34)-(37), we can obtain the ASER of the proposed scheme under gamma-gamma channel model for M -PSK modulation scheme using (45).

Although the APEP expression (45) has infinite summation terms due to the use of infinite summation form of gamma-gamma channel model (52), it can provide a very accurate value of APEP for finite summation as seen in [35]–[37]. The following Lemma presents the truncation error for (45).

Lemma 3: The upper bounded of truncation error caused by eliminating the infinite terms after the first U terms of q in (45) is

$$\epsilon_R(U) \leq \frac{(2/\sqrt{\gamma})^U}{1 - (2/\sqrt{\gamma})^U} \sum_{m_1=0}^{N_1} \sum_{m_2=0}^{N_2} \binom{N_1}{m_1} \binom{N_2}{m_2} \max_{q>U} \{u_{q,r}(N_1, N_2, m_1, m_2, A_{kj}, B_{kj})\}. \quad (46)$$

where

$$\begin{aligned} & u_{q,r}(N_1, N_2, m_1, m_2, A_{kj}, B_{kj}) \\ &= \frac{G_q(N_1, N_2, m_1, m_2, A_{kj}, B_{kj})}{\Gamma\left(\frac{q+(N_1+N_2-m_2-m_1)\beta+(m_1+m_2)\alpha}{2}\right)} \\ & \times \frac{\Gamma\left(\frac{q+(N_1+N_2-m_2-m_1)\beta+(m_1+m_2)\alpha+1}{2}\right)}{(q + (N_1 + N_2 - m_2 - m_1)\beta + (m_1 + m_2)\alpha)} \\ & \times \frac{1}{\sqrt{\pi}\left(\frac{\sqrt{\gamma}}{2}\right)^{(N_1+N_2-m_2-m_1)\beta+(m_1+m_2)\alpha}}. \quad (47) \end{aligned}$$

Proof: Refer to Appendix C for a proof.

It can be observed from the above equation that the truncation error $\epsilon_R(U)$ decreases with an increase in U and/or γ . For illustration purposes, the truncation error of APEP for 2 users-based M2M-C-FSO system for which $N_1 = N_2 = 1$ is calculated hereinafter. It can be observed that for practical atmospheric fluctuation scenarios of strong and moderate turbulences, the value of $U > 25$ gives a truncation error in the order of 10^{-7} at SNR = 10 dB. In order to have minimum truncation error, we have used $U = 200$ for calculating ASER in the numerical section.

C. ASYMPTOTIC ANALYSIS AND DIVERSITY ORDER

Let us consider 2 users M2M-C-FSO system, for which $N_1 = N_2 = 1$. Therefore, using (45), the APEP can be given as

$$\begin{aligned} & \text{APEP}(A_{kj}, B_{kj}) \\ &= \sum_{q=0}^{\infty} \frac{G_q(1, 1, 0, 0, A_{kj}, B_{kj})}{\Gamma\left(\frac{q+2\beta}{2}\right)} \\ & \times \frac{\Gamma\left(\frac{q+2\beta+1}{2}\right)}{(q + 2\beta)\sqrt{\pi}\left(\frac{\sqrt{\gamma}}{2}\right)^{q+2\beta}} \end{aligned}$$

$$\begin{aligned} & + \sum_{q=0}^{\infty} \frac{G_q(1, 1, 0, 1, A_{kj}, B_{kj}) + G_q(1, 1, 1, 0, A_{kj}, B_{kj})}{\Gamma\left(\frac{q+2\beta}{2}\right)} \\ & \times \frac{\Gamma\left(\frac{q+\beta+\alpha+1}{2}\right)}{(q + \beta + \alpha)\sqrt{\pi}\left(\frac{\sqrt{\gamma}}{2}\right)^{q+\beta+\alpha}} \\ & + \sum_{q=0}^{\infty} \frac{G_q(1, 1, 1, 1, A_{kj}, B_{kj})}{\Gamma\left(\frac{q+2\alpha}{2}\right)} \frac{\Gamma\left(\frac{q+2\alpha+1}{2}\right)}{(q + 2\alpha)\sqrt{\pi}\left(\frac{\sqrt{\gamma}}{2}\right)^{q+2\alpha}}. \quad (48) \end{aligned}$$

The asymptotic APEP expression can be obtained by putting $q = 0$ in (48) and since $(\alpha + \beta) > \min(\alpha, \beta)$ the middle term can be ignored. Thus, asymptotic APEP expression can be compactly written as

$$\begin{aligned} \lim_{\gamma \rightarrow \infty} \text{APEP} &= \sum_{q=0}^{\infty} \frac{G_q(1, 1, g_1, g_2, A_{kj}, B_{kj})}{\Gamma\left(\frac{q+2\delta}{2}\right)} \\ & \times \frac{\Gamma\left(\frac{q+2\delta+1}{2}\right)}{(q + 2\delta)\sqrt{\pi}\left(\frac{\sqrt{\gamma}}{2}\right)^{q+2\delta}}, \quad (49) \end{aligned}$$

where $\delta = \min(\alpha, \beta)$ represents diversity order and $g_1 = g_2 = 1$ if $\alpha < \beta$ otherwise $g_1 = g_2 = 0$. By observing the SNR exponent in (49), it is revealed that the diversity order of the proposed scheme for 2 users is $\min(\alpha, \beta)$, which is double that of non-cooperative M2M-NC-FSO system with 2 users. Similarly for N users, the asymptotic APEP expression has the same form as given in (49). The only difference is that $\delta = (N/2)\min(\alpha, \beta)$ and $g_1 = N_1$ and $g_2 = N_2$ when $\alpha < \beta$, otherwise $g_1 = g_2 = 0$. Therefore, with N cooperative users, the diversity order of the M2M-C-FSO scheme is N time higher than the M2M-NC-FSO scheme. Note that APEP expression for gamma-gamma channel model is valid only for $A_{kj} \neq 0$ and $B_{kj} \neq 0$. Hence, the observed diversity order is valid only for the rotation angles for which A_{kj} and B_{kj} are not zero.

IV. NUMERICAL RESULTS

In this section, the derived analytical formulas are validated through Monte Carlo simulation results along with detailed discussion and comparison of the results. The values of (α, β) are chosen as (4, 1.9) and (4.2, 1.4) for moderate and strong AT conditions [2], respectively.

The analytical and simulation-based ASER curves for the two user M2M-C-FSO system are compared in Fig. 4 under log-normal channel with $\sigma = 0.2$ and different values of θ using (11) and (33) for QPSK modulation. A perfect matching between the analytical and simulation ASER curves corroborate the accuracy of the conducted performance analysis and derivations. The comparison reveals the dependency of the ASER performance on θ and explicates that the poorest ASER performance is observed for $\theta = 0$, i.e., for conventional QPSK symbol. It can be noticed from the figure that with increasing the value

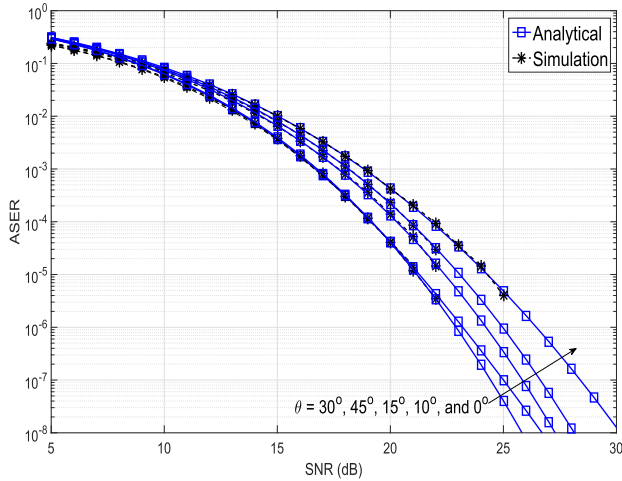


FIGURE 4. Analytical and simulation-based ASER curves of the proposed scheme for two users with different values of θ under log-normal channel with $\sigma = 0.2$.

of θ , i.e., $\theta = 10^\circ, 15^\circ, 30^\circ$, the error performance improves. Additionally, the slope for the curves associated with these values of θ is higher as compared to that observed for $\theta = 0$. This means a small rotation in the conventional QPSK symbols improves the diversity order of the proposed scheme. However, for $\theta = 45^\circ$, the slope of the error curve becomes identical to the slope of the error curve for $\theta = 0$. Furthermore, for the moderate-to-high SNR regime, it may seem that the ASER of the scheme at $\theta = 45^\circ$ is better than that observed at $\theta = 15^\circ$ and 10° , but it is not true for all values of SNR. For a very high SNR, the error performance of the proposed scheme at $\theta = 15^\circ$ and 10° will become better as compared to $\theta = 45^\circ$. This is because for $\theta = 45^\circ$, rotated QPSK symbol cannot be represented uniquely either from the in-phase or the quadrature component.

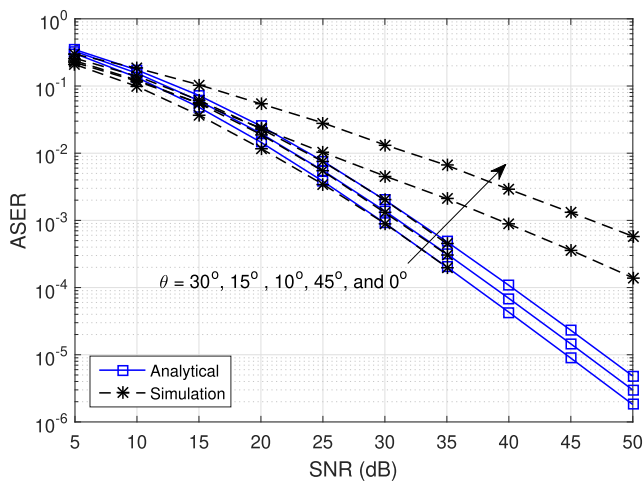


FIGURE 5. Analytical and simulation-based ASER curves of the proposed M2M-C-FSO scheme for two users with different values of θ under strong AT condition.

Similar comparison is illustrated in Fig. 5 over gamma-gamma channel using (11) and (45). The matching of analytical and simulation results curves verifies the correctness

of the derived analytical expressions. Since the values of A_{kj} and B_{kj} cannot be 0 in the derived expression, there is no analytical-based ASER curve for $\theta = 0$ and $\theta = 45^\circ$. Similar to the log-normal channel, the ASER performance is highly dependent on the value of θ . Also, the worst error performance under gamma-gamma channel is observed at $\theta = 0$, followed by $\theta = 45^\circ$. Since the diversity order under gamma-gamma channel model is finite, the error curves of $\theta = 0$ and $\theta = 45^\circ$ can be easily observed distinctly from other error curves, which have higher diversity. The diversity order can be determined by calculating the slope of the error curves at high SNR. For $\theta = 0$ and 45° , the diversity order will be $\min(\alpha, \beta)/2$, whereas for all other values of θ , the diversity order will be doubled and will equal $\min(\alpha, \beta)$. The same diversity order has been observed in the asymptotic analysis of APEP (cf. (49)). This shows that in the proposed M2M-C-FSO scheme, the diversity order can be improved by transmitting the rotated QPSK constellation symbol ($0 < \theta < 45^\circ$) instead of transmitting the traditional QPSK symbol.

Remark 1: The concept of SSD can increase the diversity order of the M2M-C-FSO scheme. However, for some values of θ , the diversity order of the proposed cooperative scheme will be similar to the diversity order observed for $\theta = 0$. Therefore, the choice of θ becomes an important parameter.

Since the ASER of the proposed scheme heavily depends on θ , there must be some optimum value of θ , termed as θ_{opt} , at which the ASER is minimum. Under log-normal channel model, the optimum value of θ is dependent on SNR, i.e., the optimum value of θ is different for moderate SNR and high SNR regimes. This can be easily observed from Fig. 4, where for the moderate values of SNR, 45° is an optimum choice of θ ; whereas for high SNR, $\theta = 30^\circ$ gives the lowest ASER. Therefore, under the log-normal channel, the θ_{opt} depends on SNR. In order to obtain θ_{opt} for rotated QPSK modulation symbol, the ASER of the scheme is numerically evaluated using (11) and (33) for $0 \leq \theta \leq 45^\circ$. After that, the minimum value of the ASER and its corresponding θ is determined for different values of SNR. The values of θ_{opt} for different values of SNR and σ is provided in Table 1, which indicates that the values of θ_{opt} depend on both the SNR and σ . However, for gamma-gamma channels, since all the curves are parallel in the moderate-to-high SNR regime (cf. Fig. 5), the value of θ_{opt} is independent of SNR. In order to find θ_{opt} , the ASER with respect to different value of θ is illustrated in Fig. 6 for QPSK and 8-PSK constellations at SNR = 80 dB using (11) and (45). The convex nature of ASER with respect to θ is observed in the figure and the minimum ASER occurs at $\theta = 29^\circ$ and $\theta = 30^\circ$ under strong and moderate AT conditions, respectively, while considering QPSK modulation. This shows that the optimal value of θ depends on the turbulence condition. Similarly, for 8PSK modulation, the values of θ_{opt} change and it is 8° and 7° for strong and moderate AT, respectively.

Remark 2: The value of θ_{opt} depends on SNR for log-normal channel model whereas, it is independent of SNR for the gamma-gamma channel model. Also, the optimum

TABLE 1. θ_{opt} for QPSK constellation under weak AT condition.

SNR	$\sigma = 0.1$	$\sigma = 0.2$	$\sigma = 0.3$
50	35°	30°	30°
60	45°	25°	30°
70	N/A	35°	30°
80	N/A	35°	65°

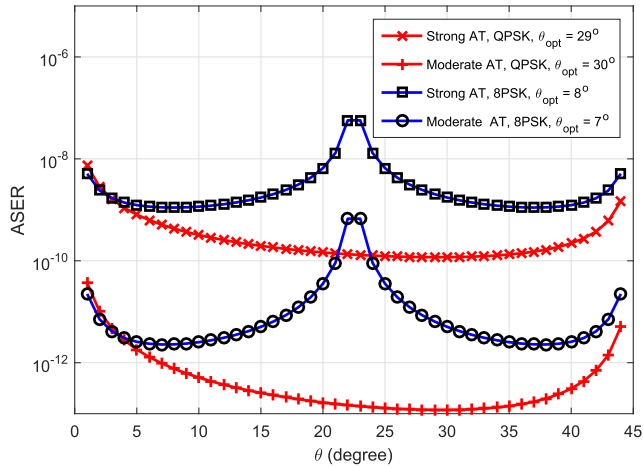


FIGURE 6. ASER as a function of θ for different turbulence regimes and modulation order.

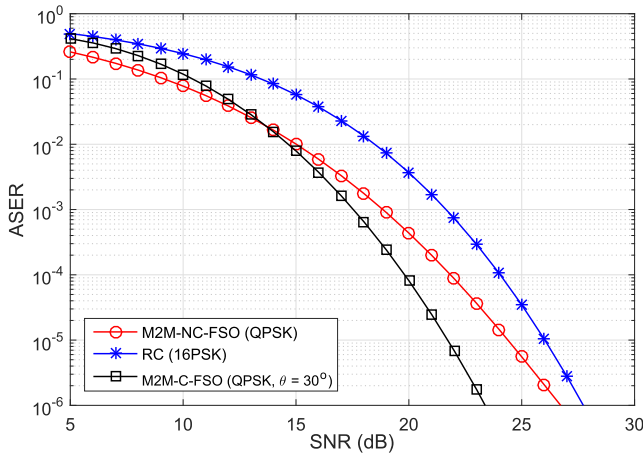


FIGURE 7. Comparison of error performance of M2M-C-FSO, M2M-NC-FSO and RC schemes at spectral efficiency of 4 bits/sec/Hz under log-normal channel model with $\sigma = 0.2$.

value of θ depends on the considered modulation order of PSK.

The comparison of different possible transmission schemes in M2M-FSO system is illustrated in Figs. 7 and 8 for two users over log-normal and gamma-gamma channel models, respectively. The different considered schemes in these figures are RC [38], M2M-NC-FSO [39], [40], and the proposed M2M-C-FSO schemes. Note that the y-axis in these figure denotes ASER of the overall system. In order to maintain the same throughput for all the considered schemes, M2M-NC-FSO and M2M-C-FSO employ QPSK signal constellation whereas RC uses 16-PSK signal constellation.

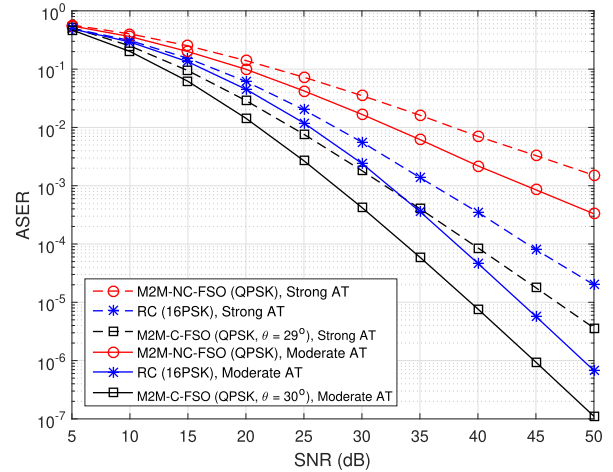


FIGURE 8. Comparison of error performance of M2M-C-FSO, M2M-NC-FSO and RC schemes at spectral efficiency of 4 bits/sec/Hz under gamma-gamma channel model.

In this way, 4 bits are transmitted in each transmission in all considered schemes, i.e., all the schemes shown in these figures have spectral efficiency of 4 bits/sec/Hz. The illustrated comparison in Fig. 7 is performed at $\sigma = 0.2$ for two users using (11), (14), and (33). It can be observed from this figure that under low SNR regime, the error performance of the M2M-NC-FSO scheme outperforms M2M-C-FSO scheme. However, with increasing SNR, the proposed M2M-C-FSO scheme outperforms M2M-NC-FSO. This is because the diversity order of the proposed M2M-C-FSO scheme is twice the diversity of the M2M-NC-FSO scheme. On the other hand, M2M-C-FSO scheme performs better than the RC scheme for all values of SNR. A similar kind of comparison over gamma-gamma channel model is illustrated in Fig. 8 using (11), (14), and (45). It can be noticed from the figure that the minimum diversity order is viewed in M2M-NC-FSO, which is equivalent to the diversity order of a SISO link. On the other hand, the diversity order of RC and the proposed M2M-C-FSO scheme is similar. Therefore, there is no benefit in using M2M-NC-FSO scheme since it gives worst ASER performance as compared to the other two schemes. Furthermore, although M2M-C-FSO and RC schemes attain the same diversity, the proposed scheme outperforms RC by 5 dB in strong AT regime and by 4.5 dB in moderate AT regime. This shows that the proposed M2M-C-FSO system provides the best possible ASER performance in M2M-FSO set-up. Also, each user can attain the maximum possible diversity. In Fig. 9, a comparison of the considered schemes is displayed for a spectral efficiency of 6 bits/sec/Hz over gamma-gamma channel model. The M2M-C-FSO and M2M-NC-FSO schemes employ 8PSK modulation [40], whereas RC uses 64PSK modulation [38]. In this way, it is clear that the proposed M2M-C-FSO scheme uses a modulation order similar to the modulation order of M2M-NC-FSO scheme. Also, the RC scheme needs a much higher modulation order than M2M-C-FSO

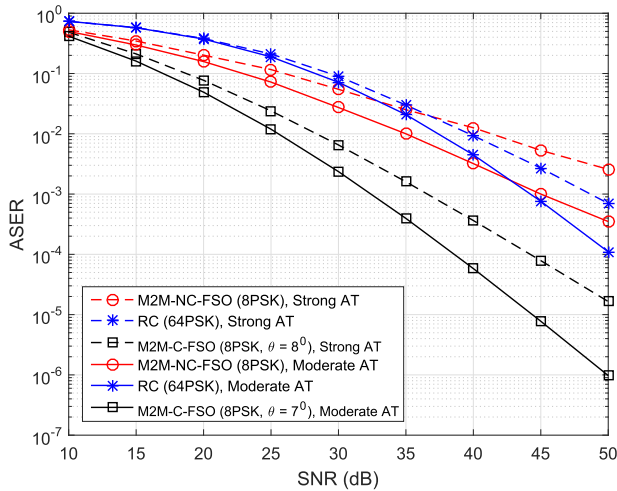


FIGURE 9. Comparison of error performance of M2M-C-FSO, M2M-NC-FSO and RC schemes at spectral efficiency of 6 bits/sec/Hz under gamma-gamma channel model.

and M2M-NC-FSO schemes for transmitting at the same spectral efficiency. Furthermore, it can be observed from the figure that contrary to 4 bits/sec/Hz scenario (cf. Fig. 8), the error performance of M2M-NC-FSO scheme outperforms the error performance of RC for low-to-moderate SNR regime at 6 bits/sec/Hz. However, due to the higher diversity order of RC, at moderate-to-high SNR regime, the error performance of RC outperforms M2M-NC-FSO scheme. It is interesting to note that the proposed M2M-C-FSO scheme outperforms RC and M2M-NC-FSO schemes for all regimes of SNR. This implies that for higher spectral efficiency, the RC may perform poorer than M2M-NC-FSO scheme but the proposed M2M-C-FSO always performs better than the other two schemes.

Remark 3: The proposed cooperative scheme has N times higher diversity order as compared to non-cooperative scheme and it outperforms RC scheme under all considered channel models.

Remark 4: The proposed cooperative scheme requires the same modulation order as that of the modulation order of the users' information signal.

Another way to attain optimum error performance is to use perfect STBC given in [41]. Fig. 10 compares the performance of the systems employing M2M-C-FSO and perfect STBC for 2×2 system. As evident in the figure, both schemes demonstrate alike error performance. However, using the proposed M2M-C-SSD promises several advantages over perfect STBC. First, perfect STBC performs joint detection to decode the users' symbols; whereas M2M-C-SSD scheme decodes the symbols individually. As such, the receiver computational complexity is much higher in perfect STBC as compared to M2M-C-SSD. For instance and considering 2×2 system with M modulation order, perfect STBC requires M^2 searches, while M2M-C-SSD involves only $2M$ searches. Second, for a 2×2 system, the proposed M2M-C-FSO enables each user to decode its

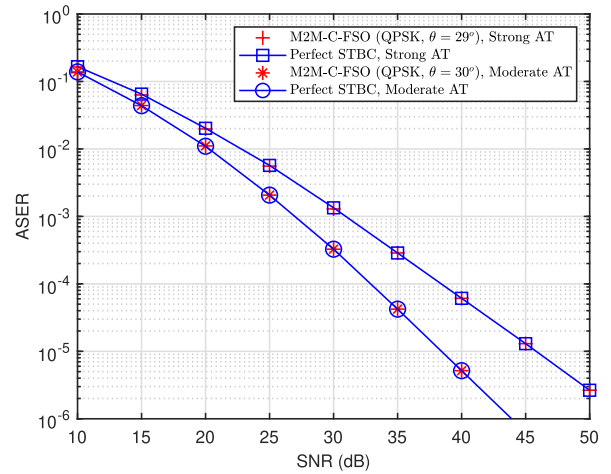


FIGURE 10. Comparison of error performance of M2M-C-FSO and Perfect STBC for 2×2 system under gamma-gamma channel model.

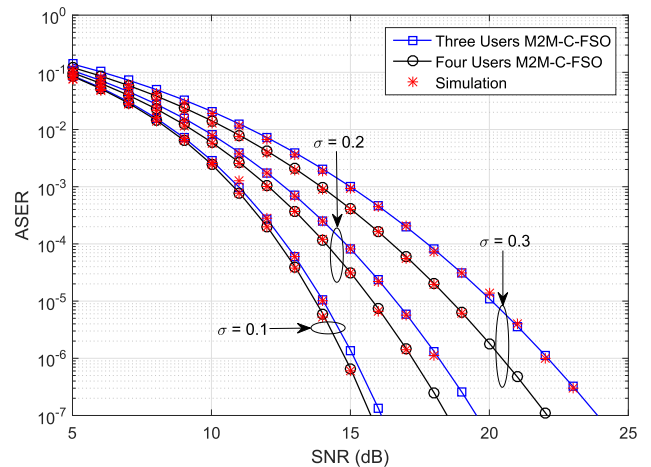


FIGURE 11. Comparison of error performance of three and four users M2M-C-FSO scheme under different values of σ .

symbol at each time interval; while users in perfect STBC decode their symbols only after the whole STBC is received. In general, for $N \times N$ system, the user needs to wait for N time intervals in the system employing perfect STBC for decoding its symbol. Yet, the user can decode its symbols after $\lceil N/2 \rceil$ time intervals in the proposed system employing M2M-C-FSO. Third, the encoding complexity in perfect STBC is substantially higher than that of M2M-C-FSO, since designing a perfect STBC for an arbitrary number of users is not straight forward. In summary, it can be concluded that the proposed M2M-C-FSO scheme significantly reduces the overall system complexity as compared to the perfect STBC while maintaining identical error performance.

A comparison of the ASER for three and four users M2M-C-FSO scheme over the log-normal channel with different values of σ at $\theta = 30^\circ$ is illustrated in Fig. 11. Since the diversity order over the log-normal channel is infinite, there is not much difference observed in the slope of the curve between the three and four users schemes. It can be noticed that increasing the number of users to four instead of three causes negligible impact on the ASER performance at low

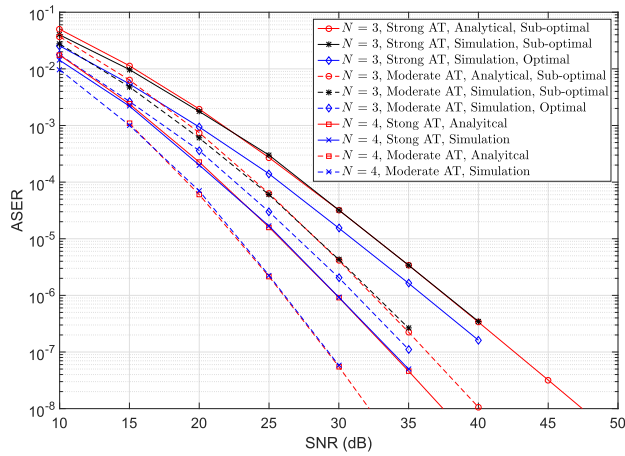


FIGURE 12. Comparison of error performance of three and four users M2M-C-FSO scheme under moderate (with $\theta = 30^\circ$) and strong AT conditions (with $\theta = 29^\circ$).

values of σ . For example, at $\sigma = 0.1$, four users system requires 0.3 dB more SNR to achieve a BER of 10^{-7} as compared to three users system. However, the gap increases with increasing the value of σ . A similar comparison over gamma-gamma channel model is illustrated in Fig. 12. Since the derived expression (45) provides the sub-optimal values for odd number of users, there are two simulation-based ASER curves corresponding to optimal (18) and sub-optimal (40) ML detector, depicted in the figure for three users based M2M-C-FSO scheme. It can be observed from the figure that there is around 1 dB SNR difference between exact and sub-optimal ML decoder based ASER curves, which is not substantial. Thus, for odd number of users, the derived expression provides an upper-bound expression of the proposed scheme. However, for even number of users, the derived expression is for optimal ML detection. It can be easily observed from the figure that increasing the number of users in the cooperative scheme enhances the diversity order of each user. This implies that by sharing the resources, each user can achieve the targeted ASER with less power as compared to that when the users are operating in non-cooperative manner. The diversity order can be determined by calculating the slope of the error curves at high SNR, which will be $(N/2) \min(\alpha, \beta)$. The diversity order of the system can be evaluated graphically by calculating the slope of ASER over a 10 dB SNR range at high SNR values. As an example, for 3 users-based M2M-C-FSO system in strong turbulence condition, ABER at SNR = 35 dB is 3.2×10^{-8} , while it is 3.4×10^{-6} at 45 dB. Therefore, the diversity order will be $\log_{10}((3.4 \times 10^{-6})/(3.2 \times 10^{-9})) = 2.03$. On the other hand, the analytical diversity order is $\delta = (N/2) \min(\alpha, \beta) = 1.5 \min(4.2, 1.4) = 2.1$. In addition, for 3 users-based system, the analytical diversity order is 2.69 and the graphical diversity order is 2.85 in the moderate turbulence condition. In the case of 4 users-based system, the analytical diversity order is 2.78 and 3.61 whereas the graphical diversity order is 2.8 and 3.8 for strong and moderate turbulence conditions, respectively.

These results corroborate the accuracy of the conducted analysis for diversity order.

Remark 5: With increasing number of users in M2M-C-FSO scheme, the error performance of each users improves under all the considered channel models.

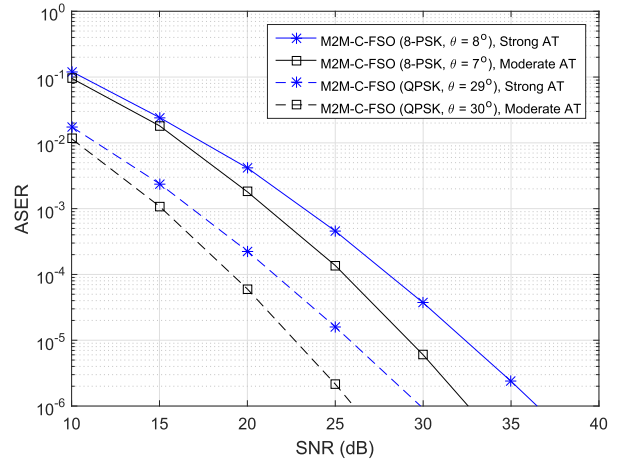


FIGURE 13. Comparison of error performance of different rates four users M2M-C-FSO scheme under moderate and strong AT conditions.

A comparison of error performance for 4 users-based M2M-C-FSO scheme having different spectral efficiency is illustrated in Fig. 13. The considered spectral efficiencies are 4 bits/sec/Hz and 6 bits/sec/Hz using QPSK and 8-ary PSK modulation, respectively. It can be observed from the figure that increasing the spectral efficiency causes degradation in error performance under both strong and moderate turbulence conditions. This shows the trade-off between spectral efficiency and ASER. In addition, the Fig. 13 along with Figs. 8 and 9 shows that the proposed scheme can be used for arbitrary modulation order and arbitrary number of users/channels.

TABLE 2. Comparison of the proposed M2M-C-FSO and clusters-based M2M-FSO [17] in terms of diversity order of the overall system for $\beta < \alpha$.

N	Proposed M2M-C-FSO	Clustered-based M2M-FSO [17]
2	β	β
3	1.5β	1.5β
4	2β	1.5β
5	2.5β	2β

The comparison of the proposed M2M-C-FSO system and cluster-based M2M-FSO system in terms of the diversity order of the overall system is illustrated in Table 2 for different numbers of users N . The diversity order for optimal grouping (given in [17, Table 1]) is considered for the cluster-based M2M-FSO system. It can be observed from the table that the diversity order of both schemes is the same for $N = 2$ and 3. However, for a higher number of N , the diversity order of the proposed scheme is better as compared to that observed in [17]. This concludes that for a higher number of users the proposed M2M-C-FSO scheme

is more efficient as compared to clusters-based M2M-FSO scheme.

V. CONCLUSION

A novel multi-point to multi-point cooperative FSO system is proposed by utilizing the concept of signal space diversity. The analytical expressions of the ASER of the proposed scheme under log-normal and gamma-gamma channel models have been evaluated and corroborated through Monte Carlo simulation results. It has been observed that the proposed M2M-C-FSO scheme significantly outperforms M2M-NC-FSO and RC schemes over wide range of system and channel parameters. Besides, it is reported that the diversity order attained by a particular user improves with increasing the number of collaborative users. Furthermore, the optimal rotation angles have been found numerically for different turbulence regimes and modulation orders. A future extension of this work may include the study of the proposed schemes under MIMO configurations. The study of the effect of pointing-error on the performance of the proposed set-up can be seen as another interesting research problem.

**APPENDIX A
PROOF OF LEMMA 1**

Using (9), the PEP can be expressed as

$$\begin{aligned} & \text{PEP}^{s_1 \rightarrow \hat{s}_1^k} \\ &= \Pr \left\{ \left[(\Re(y_1) - PR\xi h_1 \Re(\hat{s}_1^k))^2 \right. \right. \\ & \quad \left. \left. + (\Im(y_2) - PR\xi h_2 \Im(\hat{s}_1^k))^2 \right] < \left[(\Re(y_1) - PR\xi h_1 \Re(s_1))^2 \right. \right. \\ & \quad \left. \left. + (\Im(y_2) - RP\xi h_2 \Im(s_1))^2 \right] \right\}, \end{aligned} \tag{50}$$

where $\Re(y_1) = R\xi h_1 \Re(s_1) + \Re(n_1)$, $\Im(y_2) = R\xi h_2 \Im(s_1) + \Im(n_2)$. After some algebraic simplification, we have

$$\begin{aligned} \text{PEP}^{s_1 \rightarrow \hat{s}_1^k} &= \Pr \left\{ \frac{PR\xi}{2} \left[h_1^2 (\Re(\hat{s}_1^k) - \Re(s_1))^2 \right. \right. \\ & \quad \left. \left. + h_2^2 (\Im(\hat{s}_1^k) - \Im(s_1))^2 \right] < C \right\}, \end{aligned} \tag{51}$$

where $C = \left[\Re(n_1)h_1 (\Re(\hat{s}_1^k) - \Re(s_1)) + \Im(n_2)h_2 (\Im(\hat{s}_1^k) - \Im(s_1)) \right]$ with $\text{mean}(C) = 0$ and $\text{var}(C) = \frac{\sigma_n^2}{2} \left[h_1^2 (\Re(\hat{s}_1^k) - \Re(s_1))^2 + h_2^2 (\Im(\hat{s}_1^k) - \Im(s_1))^2 \right]$, the PEP can be expressed as given in (12).

**APPENDIX B
PROOF OF LEMMA 2**

The distribution of h_i under gamma-gamma channel model given in (16) can be represented in infinite series form as [36, Eq. (9)]

$$f_{h_i}(h_i) = \sum_{q=0}^{\infty} a_q(\alpha, \beta) h_i^{q+\beta-1} + \sum_{q=0}^{\infty} a_q(\beta, \alpha) h_i^{q+\alpha-1}, \tag{52}$$

where

$$a_q(\alpha, \beta) = \frac{(\alpha\beta)^{\beta+q} \Gamma(\alpha - \beta)}{\Gamma(\alpha) \Gamma(\beta) q! (1 + \beta - \alpha)_q}, \tag{53}$$

with $(1 + \beta - \alpha)_q$ being the Pochhammer symbol. The convergence test for the above infinite series is also provided in [36]. All further expressions of error performance of the proposed scheme are obtained by using the converging integrals and series manipulations of (52), therefore, these error performance results are also converging. After using transformation of random variable, the pdf of $y_i = h_i^2$ is obtained as

$$f_{y_i}(y_i) = \sum_{q=0}^{\infty} \frac{a_q(\alpha, \beta)}{2} y_i^{\frac{q+\beta}{2}-1} + \sum_{q=0}^{\infty} \frac{a_q(\beta, \alpha)}{2} y_i^{\frac{q+\alpha}{2}-1}. \tag{54}$$

The MGF of y_i is given by

$$M_{y_i}(-s) = \sum_{q=0}^{\infty} b_q(\alpha, \beta) s^{-\frac{q+\beta}{2}} + \sum_{q=0}^{\infty} b_q(\beta, \alpha) s^{-\frac{q+\alpha}{2}}, \tag{55}$$

where $b_q(\alpha, \beta) = \frac{a_q(\alpha, \beta)}{2} \Gamma\left(\frac{q+\beta}{2}\right)$. Now, the MGF of the RV $x_{N'} = \sum_m^{N'} y_m$ is given by

$$\begin{aligned} M_{x_{N'}}(-s) &= (M_{y_m}(-s))^{N'} \\ &= \sum_{m=0}^{N'} \binom{N'}{m} \left(\sum_{q=0}^{\infty} b_q(\alpha, \beta) s^{-\frac{q+\beta}{2}} \right)^{N'-m} \\ & \quad \times \left(\sum_{q=0}^{\infty} b_q(\beta, \alpha) s^{-\frac{q+\alpha}{2}} \right)^m \\ &= \sum_{m=0}^{N'} \binom{N'}{m} \sum_q^{\infty} c_q(N' - m, m) s^{-\frac{q+(N'-m)\beta+m\alpha}{2}}, \end{aligned} \tag{56}$$

where $c_q(\mu, \nu) = b_q^{(\mu)}(\alpha, \beta) * b_q^{(\nu)}(\beta, \alpha)$ and $b_q^{(\mu)}(\alpha, \beta)$ means that $b_q(\alpha, \beta)$ is convolved $\mu - 1$ times with itself, e.g., $b_q^{(2)}(\alpha, \beta) = b_q(\alpha, \beta) * b_q(\alpha, \beta)$ and $b_q^{(0)}(\alpha, \beta) = 1$. The pdf of $x_{N'}$ is therefore expressed as

$$\begin{aligned} f_{x_{N'}}(x_{N'}) &= \sum_{m=0}^{N'} \binom{N'}{m} \sum_{q=0}^{\infty} c_q(N' - m, m) \\ & \quad \times \frac{x_{N'}^{\frac{q+(N'-m)\beta+m\alpha}{2}-1}}{\Gamma\left(\frac{q+(N'-m)\beta+m\alpha}{2}\right)}. \end{aligned} \tag{57}$$

Let $w_{A_{kj}} = A_{kj} x_{N'}$ with $N' = \lceil N/2 \rceil$, then the pdf of $w_{A_{kj}}$ can be obtained by transformation of RV as

$$\begin{aligned} f_{w_{A_{kj}}}(w_{A_{kj}}) &= \sum_{m=0}^{\lceil N/2 \rceil} \binom{\lceil N/2 \rceil}{m} \sum_{q=0}^{\infty} \frac{c_q(\lceil N/2 \rceil - m, m)}{\Gamma\left(\frac{q+(\lceil N/2 \rceil - m)\beta+m\alpha}{2}\right)} \\ & \quad \times \frac{w_{A_{kj}}^{\frac{q+(\lceil N/2 \rceil - m)\beta+m\alpha}{2}-1}}{A_{kj}^{\frac{q+(\lceil N/2 \rceil - m)\beta+m\alpha}{2}}}, \end{aligned} \tag{58}$$

where $A_{kj} \neq 0$. Similarly, the pdf of $w_{B_{kj}}$ can be obtained by replacing A_{kj} with B_{kj} and $\lceil N/2 \rceil$ by $\lfloor N/2 \rfloor$ into (58). At last,

since $z' = w_{A_{kj}} + w_{B_{kj}}$, the MGF of z can be written as

$$M_{z'}(-s) = \left[\sum_{m_1=0}^{N_1} \binom{N_1}{m_1} \sum_{q=0}^{\infty} \frac{c_q(N_1 - m_1, m_1)}{\Gamma\left(\frac{q+(N_1-m_1)\beta+m_1\alpha}{2}\right)} \times \frac{w_1^{\frac{q+(N_1-m_1)\beta+m_1\alpha}{2}-1}}{A_{kj}^{\frac{q+(N_1-m_1)\beta+m_1\alpha}{2}}} \right] \times \left[\sum_{m_2=0}^{N_2} \binom{N_2}{m_2} \sum_{q=0}^{\infty} \frac{c_q(N_2 - m_2, m_2)}{\Gamma\left(\frac{q+(N_2-m_2)\beta+m_2\alpha}{2}\right)} \times \frac{w_2^{\frac{q+(N_2-m_2)\beta+m_2\alpha}{2}-1}}{B_{kj}^{\frac{q+(N_2-m_2)\beta+m_2\alpha}{2}}} \right], \quad (59)$$

where $N_1 = \lceil N/2 \rceil$ and $N_2 = \lfloor N/2 \rfloor$, which can be reduced to the following:

$$M_{z'}(-s) = \sum_{m_1=0}^{N_1} \sum_{m_2=0}^{N_2} \binom{N_1}{m_1} \binom{N_2}{m_2} \times \sum_{q=0}^{\infty} G_q(N_1, N_2, m_1, m_2, A_{kj}, B_{kj}) \times s^{-\frac{q+(N_1+N_2-m_1-m_2)\beta+(m_1+m_2)\alpha}{2}}, \quad (60)$$

where $G_q(N_1, N_2, m_1, m_2, A_{kj}, B_{kj}) = E_q(N_1, m_1, A_{kj}) * E_q(N_2, m_2, B_{kj})$ and $E_q(N_1, m_1, A_{kj}) = \frac{c_q(N_1-m_1, m_1)}{A_{kj}^{\frac{q+(N_1-m_1)\beta+m_1\alpha}{2}}}$. The inverse Laplace transform of (60) gives the pdf of z' .

APPENDIX C TRUNCATION ERROR

In practice, finite summation terms are used in order to obtain approximate APEP. Let us consider that only first U terms in the infinite series of (45) are used to obtain approximate APEP. In this way, the truncation error caused by eliminating the infinite terms after the first U terms of q in (45) is

$$\epsilon_R(U) = \sum_{m_1=0}^{N_1} \sum_{m_2=0}^{N_2} \binom{N_1}{m_1} \binom{N_2}{m_2} \times \sum_{q=U+1}^{\infty} u_{q,r}(N_1, N_2, m_1, m_2, A_{kj}, B_{kj}) \left(\frac{\sqrt{\gamma}}{2}\right)^q \quad (61)$$

By following the procedure given in [29] and using Taylor series expansion of $x^n/(1-x)$, the truncation error can be upper bounded as (46).

REFERENCES

[1] M. A. Khalighi and M. Uysal, "Survey on free space optical communication: A communication theory perspective," *IEEE Commun. Surveys Tuts.*, vol. 16, no. 4, pp. 2231–2258, 4th Quart., 2014.

[2] Z. Ghassemlooy, W. Popoola, and S. Rajbhandari, *Optical Wireless Communications System and Channel Modelling With MATLAB*. Boca Raton, FL, USA: CRC Press, 2013.

[3] H. Elgala, R. Mesleh, and H. Haas, "Indoor optical wireless communication: Potential and state-of-the-art," *IEEE Commun. Mag.*, vol. 49, no. 9, pp. 56–62, Sep. 2011.

[4] S. M. Aghajanzadeh and M. Uysal, "Multi-hop coherent free-space optical communications over atmospheric turbulence channels," *IEEE Trans. Commun.*, vol. 59, no. 6, pp. 1657–1663, Jun. 2011.

[5] S. Kazemlou, S. Hranilovic, and S. Kumar, "All-optical multihop free-space optical communication systems," *J. Lightw. Technol.*, vol. 29, no. 18, pp. 2663–2669, Sep. 15, 2011.

[6] M. Safari and M. Uysal, "Relay-assisted free-space optical communication," *IEEE Trans. Wireless Commun.*, vol. 7, no. 12, pp. 5441–5449, Dec. 2008.

[7] M. Karimi and M. Nasiri-Kenari, "Free space optical communications via optical amplify-and-forward relaying," *J. Lightw. Technol.*, vol. 29, no. 2, pp. 242–248, Jan. 15, 2011.

[8] J. Park, E. Lee, C.-B. Chae, and G. Yoon, "Outage probability analysis of a coherent FSO Amplify-and-Forward relaying system," *IEEE Photon. Technol. Lett.*, vol. 27, no. 11, pp. 1204–1207, Jun. 1, 2015.

[9] L. Yang, X. Gao, and M.-S. Alouini, "Performance analysis of relay-assisted all-optical FSO networks over strong atmospheric turbulence channels with pointing errors," *J. Lightw. Technol.*, vol. 32, no. 23, pp. 4011–4018, Dec. 1, 2014.

[10] R. Boluda-Ruiz, A. Garcia-Zambrana, C. Castillo-Vazquez, B. Castillo-Vazquez, and S. Hranilovic, "Amplify-and-forward strategy using MRC reception over FSO channels with pointing errors," *IEEE/OSA J. Opt. Commun. Netw.*, vol. 10, no. 5, pp. 545–552, May 2018.

[11] M. R. Bhatnagar, "Performance analysis of decode-and-forward relaying in gamma-gamma fading channels," *IEEE Photon. Technol. Lett.*, vol. 24, no. 7, pp. 545–547, Apr. 1, 2012.

[12] N. D. Chatzidihamantis, D. S. Michalopoulos, E. E. Kriezis, G. K. Karagiannidis, and R. Schober, "Relay selection protocols for relay-assisted free-space optical systems," *IEEE/OSA J. Opt. Commun. Netw.*, vol. 5, no. 1, pp. 92–103, Jan. 2013.

[13] C. Abou-Rjeily, "Performance analysis of selective relaying in cooperative free-space optical systems," *J. Lightw. Technol.*, vol. 31, no. 18, pp. 2965–2973, Sep. 15, 2013.

[14] Z. Gao, H. Liu, X. Ma, and W. Lu, "Performance of multi-hop parallel free-space optical communication over gamma-gamma fading channel with pointing errors," *Appl. Opt.*, vol. 55, no. 32, pp. 9178–9184, Nov. 2016.

[15] C. Abou-Rjeily, "All-active and selective FSO relaying: Do we need inter-relay cooperation?" *J. Lightw. Technol.*, vol. 32, no. 10, pp. 1899–1906, May 15, 2014.

[16] C. Abou-Rjeily and S. Haddad, "Inter-relay cooperation: A new paradigm for enhanced relay-assisted FSO communications," *IEEE Trans. Commun.*, vol. 62, no. 6, pp. 1970–1982, Jun. 2014.

[17] C. Abou-Rjeily, "Transceiver grouping: A novel diversity method for collaborative multiuser FSO communications," *IEEE Trans. Wireless Commun.*, vol. 16, no. 1, pp. 154–168, Jan. 2017.

[18] J. Abouei and K. N. Plataniotis, "Multiuser diversity scheduling in free-space optical communications," *J. Lightw. Technol.*, vol. 30, no. 9, pp. 1351–1358, May 1, 2012.

[19] L. Yang, X. Gao, and M.-S. Alouini, "Performance analysis of free-space optical communication systems with multiuser diversity over atmospheric turbulence channels," *IEEE Photon. J.*, vol. 6, no. 2, pp. 1–17, Apr. 2014.

[20] P. Wang, N. Xiang, Q. Gao, R. Wang, L. Guo, and Y. Yang, "On the performances of n th best user selection scheme in multiuser diversity free-space optical systems over exponentiated Weibull turbulence channels," *IEEE Photon. J.*, vol. 8, no. 2, pp. 1–15, Apr. 2016.

[21] S. Zhalehpour, M. Uysal, O. A. Dobre, and T. Ngatched, "Outage capacity and throughput analysis of multiuser FSO systems," in *Proc. IEEE 14th Can. Workshop Inf. Theory (CWIT)*, St. John's, NL, Canada, Jul. 2015, pp. 143–146.

[22] S. Zhalehpour and M. Uysal, "Performance of multiuser scheduling in free space optical systems over atmospheric turbulence channels," *IET Optoelectron.*, vol. 9, no. 5, pp. 275–281, Oct. 2015.

[23] O. S. Badarneh, F. S. Almeshadi, I. S. Ansari, and X. Yang, "Wireless energy harvesting in cooperative decode-and-forward relaying networks over mixed generalized $\eta-\mu$ and $\kappa-\mu$ fading channels," *Trans. Emerg. Telecommun. Technol.*, vol. 29, no. 2, p. e3262, Feb. 2018.

[24] S. Althunibat and R. Mesleh, "Cooperative decode-and-forward quadrature spatial modulation over correlated and imperfect $\eta-\mu$ fading channels," *Wireless Netw.*, vol. 25, no. 2, pp. 689–698, Feb. 2019, doi: [10.1007/s11276-017-1585-z](https://doi.org/10.1007/s11276-017-1585-z).

[25] D. Wan, M. Wen, F. Ji, H. Yu, and F. Chen, "Non-orthogonal multiple access for cooperative communications: Challenges, opportunities, and trends," *IEEE Wireless Commun.*, vol. 25, no. 2, pp. 109–117, Apr. 2018.

[26] J. Boutros and E. Viterbo, "Signal space diversity: A power-and bandwidth-efficient diversity technique for the Rayleigh fading channel," *IEEE Trans. Inf. Theory*, vol. 44, no. 4, pp. 1453–1467, Jul. 1998.

- [27] A. Jaiswal, M. Abaza, M. R. Bhatnagar, and V. K. Jain, "An investigation of performance and diversity property of optical space shift keying-based FSO-MIMO system," *IEEE Trans. Commun.*, vol. 66, no. 9, pp. 4028–4042, Sep. 2018.
- [28] A. Jaiswal, M. R. Bhatnagar, and V. K. Jain, "Performance evaluation of space shift keying in free-space optical communication," *J. Opt. Commun. Netw.*, vol. 9, no. 2, pp. 149–160, Feb. 2017.
- [29] X. Song and J. Cheng, "Subcarrier intensity modulated MIMO optical communications in atmospheric turbulence," *IEEE/OSA J. Opt. Commun. Netw.*, vol. 5, no. 9, pp. 1001–1009, Sep. 2013.
- [30] W. O. Popoola and Z. Ghassemloooy, "BPSK subcarrier intensity modulated free-space optical communications in atmospheric turbulence," *J. Lightw. Technol.*, vol. 27, no. 8, pp. 967–973, Apr. 15, 2009.
- [31] J. Li, J. Q. Liu, and D. P. Taylor, "Optical communication using subcarrier PSK intensity modulation through atmospheric turbulence channels," *IEEE Trans. Commun.*, vol. 55, no. 8, pp. 1598–1606, Aug. 2007.
- [32] H. Moradi, H. H. Refai, and P. G. LoPresti, "A switched diversity approach for multi-receiving optical wireless systems," *Appl. Opt.*, vol. 50, no. 29, pp. 5606–5614, Oct. 2011.
- [33] M. Abramowitz and I. A. Stegun, *Handbook of Mathematical Functions With Formulas, Graphs, and Mathematical Tables*, 9th ed. New York, NY, USA: Dover, 1972.
- [34] H. Moradi, H. H. Refai, and P. G. LoPresti, "Circular MIMO FSO nodes with transmit selection and receive generalized selection diversity," *IEEE Trans. Veh. Technol.*, vol. 61, no. 3, pp. 1174–1181, Mar. 2012.
- [35] M. R. Bhatnagar and Z. Ghassemloooy, "Performance analysis of gamma-gamma fading FSO MIMO links with pointing errors," *J. Lightw. Technol.*, vol. 34, no. 9, pp. 2158–2169, May 1, 2016.
- [36] M. R. Bhatnagar, "A one bit feedback based beamforming scheme for FSO MISO system over gamma-gamma fading," *IEEE Trans. Commun.*, vol. 63, no. 4, pp. 1306–1318, Apr. 2015.
- [37] E. Bayaki, R. Schober, and R. Mallik, "Performance analysis of MIMO free-space optical systems in gamma-gamma fading," *IEEE Trans. Commun.*, vol. 57, no. 11, pp. 3415–3424, Nov. 2009.
- [38] P. K. Sharma and A. Bansal, "DF MISO system with arbitrary beamforming in atmospheric turbulence and misalignment errors," *Photon. Netw. Commun.*, vol. 35, no. 2, pp. 204–209, Nov. 2017.
- [39] X. Song, F. Yang, J. Cheng, N. Al-Dhahir, and Z. Xu, "Subcarrier phase-shift keying systems with phase errors in lognormal turbulence channels," *J. Lightw. Technol.*, vol. 33, no. 9, pp. 1896–1904, May 1, 2015.
- [40] W. Gappmair and H. E. Nistazakis, "Subcarrier PSK performance in terrestrial FSO links impaired by gamma-gamma fading, pointing errors, and phase noise," *J. Lightw. Technol.*, vol. 35, no. 9, pp. 1624–1632, May 1, 2017.
- [41] F. Oggier, G. Rekaya, J.-C. Belfiore, and E. Viterbo, "Perfect space-time block codes," *IEEE Trans. Inf. Theory*, vol. 52, no. 9, pp. 3885–3902, Sep. 2006.



MOHAMED ABAZA (Senior Member, IEEE) received the B.Sc. and M.Sc. degrees in electronics and communications engineering from the Arab Academy for Science, Technology and Maritime Transport (AASTMT), Egypt, in 2009 and 2012, respectively, and the Ph.D. degree in digital communications from the Université de Bretagne Occidentale, France, in 2015. From 2009 to 2012, he was a Teaching Assistant with AASTMT. He is currently an Associate Professor with AASTMT.

He is the author of a book and a book chapter, 12 international journals, and seven international conferences. His current research interests include multiple-input multiple-output systems, relay-assisted cooperative communications, and optical wireless communications. In 2016, he selected as an outstanding reviewer for the ELSEVIER *Optics Communications*. He also served as IEEE Student Branch Consular and elevated to IEEE Senior Member in 2019. He also serves as a reviewer for IEEE, SPIE, OSA, and Elsevier journals.



MANAV R. BHATNAGAR (Senior Member, IEEE) received the M.Tech. degree in communications engineering from the Indian Institute of Technology Delhi, New Delhi, India, in 2005, and the Ph.D. degree in wireless communications from the Department of Informatics, University of Oslo, Oslo, Norway, in 2008. From 2008 to 2009, he was a Postdoctoral Research Fellow with the University Graduate Center (UNIK), University of Oslo. He held visiting appointments

with the Wireless Research Group, Indian Institute of Technology Delhi; the Signal Processing in Networking and Communications (SPINCOM) Group, University of Minnesota Twin Cities, Minneapolis, MN, USA; the Alcatel-Lucent Chair, SUPELEC, France; the Department of Electrical Computer Engineering, Indian Institute of Science, Bangalore, India; UNIK, University of Oslo; the Department of Communications and Networking, Aalto University, Espoo, Finland; and INRIA/IRISA Laboratory, University of Rennes, Lannion, France. He is currently a Professor with the Department of Electrical Engineering, Indian Institute of Technology Delhi, New Delhi, India. His research interests include signal processing for multiple-input-multiple-output systems, cooperative communications, non-coherent communication systems, distributed signal processing for cooperative networks, multiuser communications, ultrawideband-based communications, free-space optical communication, cognitive radio, software defined radio, power line communications, and satellite communications. He was selected as an Exemplary Reviewer of the IEEE COMMUNICATIONS LETTERS for 2010 and 2012, and an Exemplary Reviewer of the IEEE TRANSACTIONS ON COMMUNICATIONS for 2015. He was an Editor of the IEEE TRANSACTIONS ON WIRELESS COMMUNICATIONS during 2011–2014. He has received the NASI-Scopus Young Scientist Award 2016 in engineering category and the Shri Om Prakash Bhasin Award in the field of Electronics and Information Technology for the year 2016. He is a Fellow of the Institution of Engineering and Technology (IET), U.K., the Indian National Academy of Engineering (INAE), the Institution of Electronics and Telecommunication Engineers (IETE), India, and the Optical Society of India (OSI).



RAED MESLEH (Senior Member, IEEE) received the Ph.D. degree from Jacobs University, Bremen, Germany, in 2007. He is currently the Dean of the School of Electrical Engineering and Information Technology, German Jordanian University, Amman, Jordan. From 2007 to 2010, he was a Postdoctoral Fellow with Jacobs University. He was with the Electrical Engineering Department, University of Tabuk, Saudi Arabia, from 2010 to 2015. In December 2016, he was awarded

the Arab Scientific Creativity award from Arab Thought Foundation. . . .



ANSHUL JAISWAL (Member, IEEE) received the B.E. degree (Hons.) in electronics and telecommunication engineering from Chhattisgarh Swami Vivekananda Technical University, Chhattisgarh, India, in 2012, and the M.Tech. degree in opto-electronics and optical communication engineering and the Ph.D. degree in optical wireless communication from the Indian Institute of Technology Delhi, New Delhi, India, in 2015 and 2019, respectively. He worked as a Visiting

Assistant Professor with the Department of Electronics Engineering, Indian Institute of Technology (Indian School of Mines) Dhanbad, India, from August 2019 to September 2019. He is currently an Assistant Professor with the Department of Electronics and Communication Engineering, Indian Institute of Technology Roorkee, India. His research interests include optical wireless communications, multiple-input-multiple-output systems, channel modeling for wireless communications, multiple access schemes, and cooperative communication. He has secured 24th rank all over India in Joint CSIR-UGC test for the Junior Research Fellow in the subject of engineering science under CSIR fellowship scheme, in 2012. He was in top 0.25% students in graduate aptitude test in engineering in the subject of electronics and telecommunication in 2013. He serves as a Reviewer for IEEE, OSA, and Elsevier journals.